

Fig. 3 Fuel consumption reduction ratio of tumble orbit transfer compared to docked orbit transfer.

where the rotational phase has advanced by 180 deg from the instant of the impulse application. Note that the velocity increment for mass 2 is twice as large as that of the system. If the masses are separated at this instance, the apogee increment is twice as high. Mass 1, or the service vehicle, will stay in an orbit slightly different from the original circular orbit. If both masses are identical,  $\gamma_1 = \gamma_2 = 0.5$ , then mass 1 remains in the original orbit.

### III. Fuel Consumption

It was shown in the previous section that the fuel consumption in putting the dumb satellite into a new orbit is exactly half of what is required in a normal orbit transfer. Assuming further that the service vehicle returns to the original circular orbit after separation, total fuel consumption in terms of the velocity increment of the service vehicle is obtained. In the case of circular orbit injection, mass 1 must be accelerated again to the Hohmann orbit, whose perigee path is tangential to the original circular orbit. Therefore, mass 1 requires two impulses in the return journey. Velocity increments are  $\gamma_2 \Delta V_1$  and  $\gamma_1 \Delta V_1$ , respectively. Including the first maneuver, the total velocity increment of the service vehicle is  $2\Delta V_1$ .

Elliptical orbit injection requires a simpler maneuver. The required impulse is  $|\gamma_1 - \gamma_2| \Delta V_1$  at the perigee to adjust to the circular velocity. The total velocity increments are

$$[1 + (\gamma_1 - \gamma_2)] \Delta V_1 = 2\gamma_1 \Delta V_1 \quad (\gamma_1 > \gamma_2) \quad (8)$$

$$[1 + (\gamma_1 - \gamma_2)] \Delta V_1 = 2\gamma_1 \Delta V_1 \quad (\gamma_1 < \gamma_2) \quad (9)$$

To show the advantages of tumble orbit transfer, velocity increments required for an ordinary docked mode are also calculated. The docked system requires two impulses of  $\Delta V_1$  each to reach the circular orbit of radius  $R_a$ . The return journey will also require two impulses, each requiring  $\gamma_1 \Delta V_1$ . The total velocity increment is  $2(1 + \gamma_1) \Delta V_1$ . To inject the dumb object into an elliptical orbit, identical to 2.2, the service vehicle in docked system mode imparts a velocity equivalent to  $2\Delta V_1$ . Immediately after the acceleration, the vehicle separates and decelerates by  $2\gamma_1 \Delta V_1$  to recover its original speed. The total is  $2(1 + \gamma_1) \Delta V_1$ .

The fuel requirement ratios in tumble orbit transfer compared with those of the ordinary docked transfer are shown in Fig. 3.

### IV. Discussions and Conclusions

The feasibility and usefulness of tumble orbit transfer are shown under simplified assumptions. Fuel requirements can be substantially reduced compared with conventional orbit transfers in docked configuration. In the circular orbit injection, this method is particularly attractive when the payload mass is small compared with the service vehicle mass. In an ex-

treme case, tumble transfer saves half of the fuel otherwise required. In the case of elliptical orbit injection, this method is most useful where the payload mass is similar to the service vehicle mass, saving two-thirds of the fuel.

The length  $l$  of the rod that connects the vehicle and the payload is arbitrary in theory. A very short rod or even a direct connection might look feasible. However, the rotational velocity  $\phi$  increases inversely proportionally to  $l$ . So, in actual application, the maximum  $\phi$  will be determined by considerations of allowable centrifugal load and timing capability at thruster and separation. As an example, for the velocity increment  $\Delta V_1 = 10$  m/s, the rod length  $l = 10$  m produces a load equivalent to 1 g and a rotation period of 6 s. The rod can be replaced by a long flexible tether, since only the force acting between the two masses is an axial force, and bending rigidity is not required in the connecting structure. When the rod or the tether length becomes too long, the system no longer tumbles around the center of mass. Instead, it oscillates around the local vertical by the gravity gradient moment. Under this condition, the momentum is similarly transferred from the service vehicle to the payload.

Removal of spent satellites and debris will be vital for safety and continuation of future space activities. Tumble orbit transfer will be able to provide an effective means for this purpose. The principle also will be applicable to wider classes of orbit transfer once its capability in terms of insertion precision is demonstrated by those spent satellite removal missions.

### References

1. Thomas, U., "Alternative Operational Modes and Cost of Removing Geostationary Satellite Debris," *Earth-Oriented Applications of Space Technology*, Vol. 6, No. 3, 1986, pp. 307-313.

Kerry T. Nock  
Associate Editor

## Conversion of Omnidirectional Proton Fluxes into a Pitch Angle Distribution

Gautam D. Badhwar\* and Andrei Konradi†  
NASA Johnson Space Center, Houston, Texas 77058

### Introduction

WITH the anticipated long-duration radiation exposures of astronauts in an oriented space station, accurate prediction of expected doses requires consideration of both the mass distribution of the spacecraft and the direction of the incident high-energy proton flux. The two components of the directionality of the high-energy proton radiation are the highly peaked local pitch-angle distribution and the east-west effect. Since the omnidirectional flux at some point along a field line is an integral over the pitch angle distribution, in principle, an inversion of this integral should yield the desired

Received Aug. 25, 1989; revision received Nov. 9, 1989. Copyright © 1990 American Institute of Aeronautics and Astronautics, Inc. No copyright is asserted in the United States under Title 17, U.S. Code. The U.S. Government has a royalty-free license to exercise all rights under the copyright claimed herein for Governmental purposes. All other rights are reserved by the copyright owner.

\*Physicist, Space Science Branch, Solar System Exploration Division, Space and Life Sciences Directorate.

†Physicist, Space Science Branch, Solar System Exploration Division, Space and Life Sciences Directorate. Senior Member AIAA.

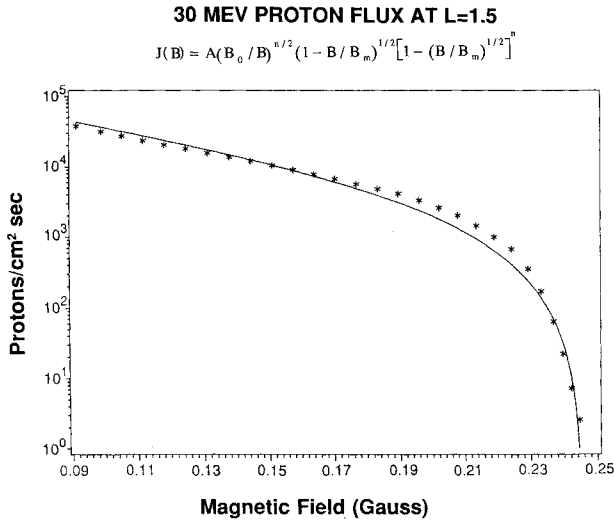


Fig. 1 Least-squares fit of a three-parameter omnidirectional proton flux (solid line) to the AP-8 MIN model (asterisks).

pitch angle distribution. We have devised a semianalytical scheme to use the omnidirectional proton fluxes of the AP-8 model<sup>1</sup> to extract time-averaged, pitch-angle distributions of high-energy protons. The results compare well with the experimental data obtained by several satellites.

### Analysis

If we know  $J(B, L)$ , the omnidirectional flux as a function of the magnetic field and the  $L$  parameter, we have a complete description of the pitch angle distribution of particles at all points along the magnetic field line.<sup>2-4</sup>

We can write the omnidirectional flux

$$J(B, L) = 2 \int_0^{\pi/2} j(\alpha, B, L) 2\pi \sin \alpha d\alpha \quad (1)$$

where  $J(B, L)$  is the omnidirectional flux at magnetic field  $B$  and McIlwain's drift shell parameter  $L$ . The local-pitch angle distribution is  $j(\alpha, B, L)$ , and  $\alpha$  is the pitch angle.

Using Liouville's theorem and the conservation of the first adiabatic invariant, we can write

$$j_0(\alpha_0) = j_B(\alpha)$$

and

$$\sin^2 \alpha_0 / B_0 = \sin^2 \alpha / B$$

where  $j_0$ ,  $\alpha_0$ , and  $B_0$  are the equatorial flux, pitch angle, and magnetic field, respectively.

In terms of the equatorial pitch-angle distribution, the omnidirectional flux becomes

$$J(B, L) = \frac{4\pi B}{B_0} \int_0^{\arcsin(B_0/B)} j_0(\alpha_0, L) \frac{\sin \alpha_0 (1 - \sin^2 \alpha_0)^{1/2} d\alpha_0}{[1 - (B/B_0) \sin^2 \alpha_0]^{1/2}} \quad (2)$$

Unfortunately, the inversion of this equation is not unique since an integral of any function  $h(\alpha)$  for which

$$0 = \int_0^{\arcsin(B_0/B)} h_0(\alpha_0) \frac{\sin \alpha_0 (1 - \sin^2 \alpha_0)^{1/2} d\alpha_0}{[1 - (B/B_0) \sin^2 \alpha_0]^{1/2}}$$

can be added to the right side of Eq. (2) without affecting the result.

Our original plan called for finding  $j_0(\alpha_0)$  numerically by expressing the integral in Eq. (2) as a product of the vector  $j_0(\alpha_0)$ , with a matrix  $\bar{\Omega}$  representing the solid angle

$$\bar{J}(B) = \bar{\Omega}(B, \alpha_0) \bar{j}(\alpha_0)$$

Then by inverting the solid-angle matrix and multiplying it by the vector  $\bar{J}(B)$ , one should in principle be able to obtain  $j_0(\alpha_0)$

$$\bar{\Omega}^{-1}(\alpha_0, B) \bar{J}(B) = \bar{j}(\alpha_0)$$

Unfortunately, in practice, a reasonable solution cannot be obtained without further assumptions or restrictions. Without those, the solution is mathematically accurate but often physically unreasonable. As a consequence, we chose to try a semi-phenomenological approach.

After some experimentation, we found that the omnidirectional flux  $J(B)$  calculated from AP-8 MIN can be very well described by a three-parameter expression

$$J(B) = A(B_0/B)^{n/2}(1-B/B_m)^{1/2}[1-(B/B_m)^{1/2}]^n \quad B \leq B_m$$

$$= 0 \quad B \geq B_m \quad (3)$$

where  $A$  and  $n$  are the scale and shape parameters, respectively, and  $B_m$  is the characteristic magnetic field within the atmospheric cutoff. The loss-cone angle can then be written

$$\sin \alpha_L = (B/B_m)^{1/2}$$

A typical fit for 30 MeV protons at  $L = 1.5$  is shown in Fig. 1.

Parker<sup>5</sup> proved that, for particles performing adiabatic motion, the following expression for the pitch-angle distribution must hold true

$$j(\alpha) = f(\sin^2 \alpha / B) \quad \alpha \geq \alpha_L$$

$$= g(\alpha) \quad \alpha \leq \alpha_L \quad (4)$$

Our search for a function  $j(\alpha)$  that would yield Eq. (3) when substituted in Eq. (2) was unsuccessful.

We then tried fitting Eq. (2) numerically with expressions of the following kind.

From Ref. 6:

$$j(\alpha) = K \exp[-n(\sin^2 \alpha)] \quad (5)$$

From Ref. 7:

$$j(\alpha) = K(B_0/B)^{n/2}(\sin^n \alpha - \sin^n \alpha_L) + C \quad \alpha \geq \alpha_L$$

$$= 0 \quad \alpha \leq \alpha_L \quad (6)$$

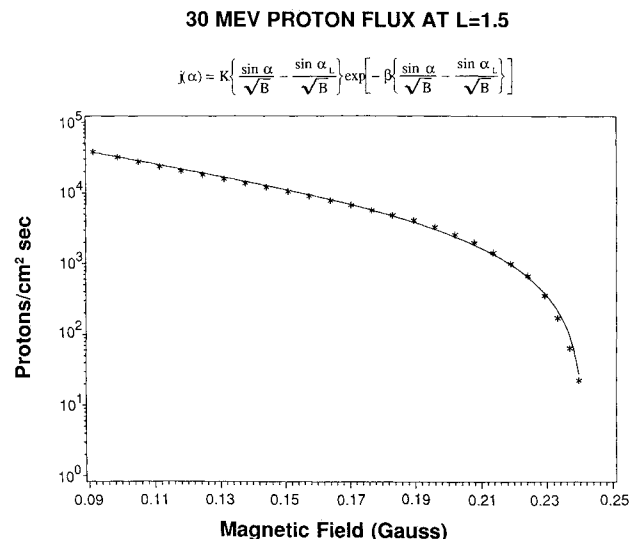


Fig. 2 Least-squares fit of a three-parameter proton, pitch-angle distribution integrated over  $4\pi$  (solid line), to the AP-8 MIN model (asterisks).

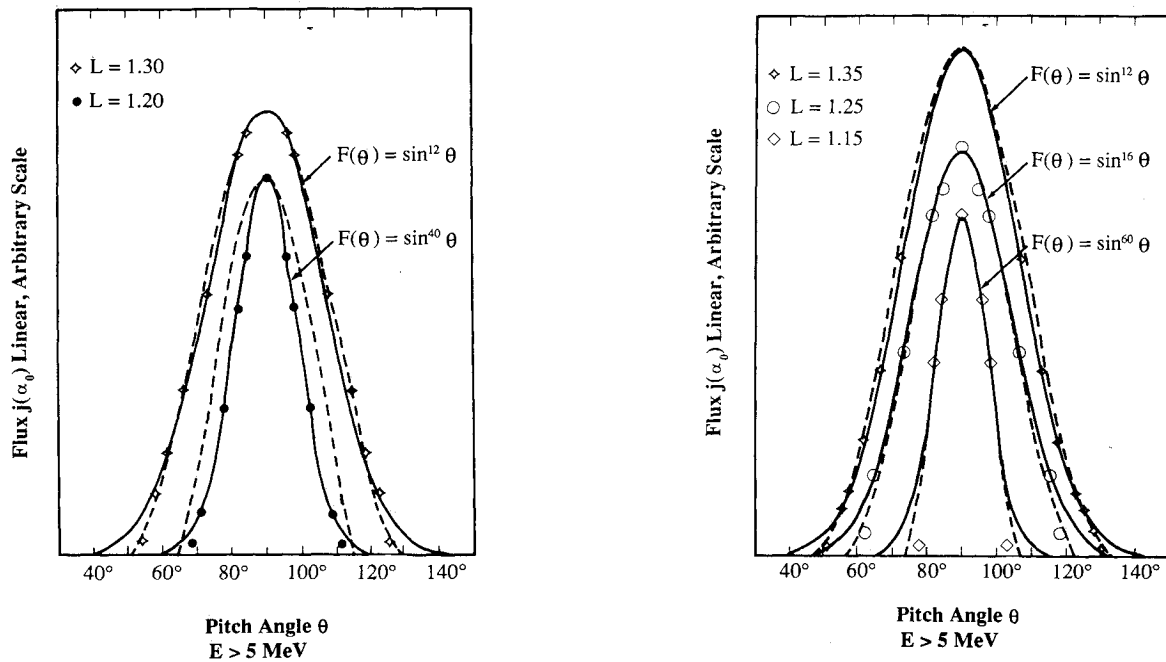


Fig. 3 Comparison of our calculated flux (dashed line) with the data (dots, circles, and diamonds) and calculations  $[F(\theta)]$  of Fischer et al.<sup>8</sup>

$$j(\alpha) = K(B_0/B)^{n/2}(\sin\alpha - \sin\alpha_L)^n + C \quad \alpha \geq \alpha_L$$

$$= 0 \quad \alpha \leq \alpha_L \quad (7)$$

Equations (5) and (6) did not yield as good a fit as Eq. (7). An expansion of Eq. (2) in terms of  $B/B_m$  using Eq. (7), and a comparison with an expansion of Eq. (3) showed that we need both even and odd terms. This led us to postulate

$$j(\alpha) = K\left(\frac{\sin\alpha}{B^{1/2}} - \frac{\sin\alpha_L}{B^{1/2}}\right) \exp\left[-\beta\left(\frac{\sin\alpha}{B^{1/2}} - \frac{\sin\alpha_L}{B^{1/2}}\right)\right] \quad \alpha \geq \alpha_L$$

$$= 0 \quad \alpha \leq \alpha_L \quad (8)$$

Expressed as an equatorial pitch-angle distribution this can be written as

$$j_0(\alpha_0) = K\left(\frac{\sin\alpha_0}{B_0^{1/2}} - \frac{1}{B_m^{1/2}}\right) \exp\left[-\beta\left(\frac{\sin\alpha_0}{B_0^{1/2}} - \frac{1}{B_m^{1/2}}\right)\right] \quad \alpha_0 \geq \alpha_{0L}$$

$$= 0 \quad \alpha_0 \leq \alpha_{0L} \quad (9)$$

where  $\alpha_0$ ,  $B_0$ ,  $B_m$ , and  $\beta$  are the equatorial pitch angle and magnetic field, the characteristic magnetic field in the region of the atmospheric cutoff, and the shape parameter.

Equation (9) produced the lowest  $\chi^2$  and the best fits to omnidirectional fluxes in AP-8 MIN as well as to experimental measurements of Fischer et al.<sup>8</sup> A typical fit is shown in Fig. 2. If we compare this to Fig. 1, it becomes clear that Eq. (9) is an excellent representation of the pitch-angle distribution.

In general, very little experimental data are available in the literature with which to compare our computational results. Figure 3 shows a comparison of our fits based on the AP-8 MIN model with experimental data of Fischer et al.<sup>8</sup> and their fit of the pitch-angle distribution to powers of the sine of the pitch angle. The fluxes have been normalized to agree at 90 deg. One should note that in most cases our fits of their inner-belt proton data are very good, especially near the loss cone, which represents the region in space where fluxes are dropping off very rapidly.

It is important to mention that the model has significant limitations. It has been known for a long time that the pitch-angle distribution of high-energy protons at low  $L$  values is highly dependent on the azimuth angle measured about the

direction of the local magnetic field. This effect is known as the east-west asymmetry, and it manifests itself in the fact that fluxes of high-energy protons traveling toward the east are higher than those of protons traveling toward the west.<sup>6,9</sup> The present study does not take this into account.

## Conclusions

We have successfully developed a scheme for deriving pitch-angle distributions of energetic protons from omnidirectional fluxes contained in the AP-8 MIN magnetospheric radiation model. We have also formulated a functional form for expressing the proton pitch-angle distributions at a given energy and  $L$  coordinate as a function of only three parameters.

## References

- <sup>1</sup>Sawyer, D. M., and Vette, J. I., "AP-8 Trapped Proton Environment for Solar Maximum and Solar Minimum," NASA/NSSDC/WDC-A-R&S 76-06, Dec. 1976.
- <sup>2</sup>Ray, E. C., "On the Theory of Protons Trapped in the Earth's Magnetic Field," *Journal of Geophysical Research*, Vol. 65, April 1960, pp. 1125-1134.
- <sup>3</sup>Lenchek, A. M., Singer, S. F., and Wentworth, R. C., "Geomagnetically Trapped Electrons from Cosmic Ray Albedo Neutrons," *Journal of Geophysical Research*, Vol. 66, Dec. 1961, pp. 4027-4046.
- <sup>4</sup>Hess, W. N., *The Radiation Belt and the Magnetosphere*, Blaisdell, Waltham, MA, 1968, pp. 63-66.
- <sup>5</sup>Parker, E. N., "Newtonian Development of the Dynamical Properties of Ionized Gases of Low Density," *Physical Review*, Vol. 107, Aug. 15, 1957, pp. 924-933.
- <sup>6</sup>Heckman, H. H., and Nakano, G. H., "East-West Asymmetry in the Flux of Mirroring Geomagnetically Trapped Protons," *Journal of Geophysical Research*, Vol. 68, April 1963, pp. 2117-2120.
- <sup>7</sup>Valot, P., and Engelmann, J., "Pitch Angle Distributions of Geomagnetically Trapped Protons for  $1.2 < L < 2.1$ ," *Space Research XIII*, Akademie Verlag, Berlin, 1973.
- <sup>8</sup>Fischer, H. M., Auschrat, V. W., and Wibberenz, G., "Angular Distribution and Energy Spectra of Protons of Energy  $5 < E < 50$  MeV at the Lower Edge of the Radiation Belt in Equatorial Latitudes," *Journal of Geophysical Research*, Vol. 82, Feb. 1977, pp. 537-547.
- <sup>9</sup>Lenchek, A. M., and Singer, S. F., "Effect of Finite Gyroradii of Geomagnetically Trapped Protons," *Journal of Geophysical Research*, Vol. 67, Sept. 1962, pp. 4073-4075.